

The evolution of additional (hidden) quantum variables in the interference of Bose-Einstein condensates

W. J. Mullin^a, R. Krotkov^a, and F. Laloë^b

^a*Department of Physics, University of Massachusetts,
Amherst, Massachusetts 01003 USA*

^b*LKB, Dept. de Physique de l'ENS,
24 rue Lhomond, 75005, Paris, France*

(Dated: December 2, 2024)

Abstract

Additional variables (also often called “hidden variables”) are sometimes added to standard quantum mechanics in order to remove its indeterminism or “incompleteness,” and to make the measurement process look more classical. Here we discuss a case in which an additional variable arises almost spontaneously from the quantum formalism: the emergence of relative phase between two highly populated Fock state Bose-Einstein condensates. The model simulated here involves the interference of two Bose condensates, one with all up spins, and the other with down spins, along a z-axis. With the clouds overlapping, we consider the results of measuring spins in a transverse plane (the general direction is studied in an appendix). The determination of the previously “hidden” phase becomes progressively more definite as additional measurements are made. We also provide an analysis of a recent and closely related experiment.

I. INTRODUCTION

Several laboratories have made use of Bose condensates with spins or pseudo-spins to perform very interesting experiments. For example, in JILA experiments^{1,2}, a mixture of two hyperfine states playing the role of pseudo-spin-1/2 particles was found to segregate by species, thereby exhibiting spin waves. Another “spin” experiment⁴ involves overlapping two Bose condensates, one with spin up and the other with spin down and observing the appearance of a spontaneous transverse spin polarization. In this paper we consider a simulation that involves the interference of two clouds of Bose gases, one with up spins and the other down spins along some z-axis. With the clouds overlapping, we consider what happens in measuring spins along a transverse direction at a set of azimuthal angles, detecting whether a spin is found up or down along each measurement angle used. (The case of a general measurement direction is studied in Appendix A.) In looking at a simulation of this process we note an interesting element involved in the process: the relation of the successive measurements to the appearance of a so-called “hidden” variable.

The introduction of additional variables to the standard formalism of quantum mechanics is not a new idea; it dates back almost to the appearance of this theory³, with, for instance, the early work of L. de Broglie⁵ and later D. Bohm on “hidden variables”⁶. The main motivation was to restore determinism by reproducing the statistical results of quantum mechanics with classical averages over additional variables. In 1935, Einstein, Podolsky and Rosen (EPR) showed that there exists an even stronger argument to complete quantum mechanics, without referring to determinism: the standard form of quantum mechanics does not satisfy local realism, and should be completed by additional “elements of reality” to restore it⁷. Thirty years later J. Bell, with a famous theorem^{8,9}, extended the EPR argument and showed that, not only the formalism, but also the predictions of quantum mechanics are sometimes incompatible with local realism. In other words, adding variables to quantum mechanics is not sufficient to restore local realism in all cases: there exist some situations where the evolution of additional variables has to be explicitly non-local. This remarkable result stimulated several generations of careful experiments in order to decide whether or not quantum mechanics still gives correct predictions, even in these surprising “non-local” situations. An impressive body of evidence has now been accumulated in favor of the predictions of quantum mechanics, even if none of these experiments is ideal¹⁰; the general

consensus among physicists is that these surprising “non-local” predictions of quantum mechanics are indeed obeyed by Nature. This does not mean that additional variables should now be excluded from quantum mechanics! Actually, advocates of these variables argue that it is precisely one of their big merits to make the non-local character of quantum mechanics explicit¹³. For a general discussion of the consequences of the Bell theorem, see for instance Refs. 11,12.

In most cases, the introduction of additional variables into quantum mechanics leaves a large range of flexibility: one has to introduce whatever new variables seem appropriate (positions, momenta, fields, etc.) with adequate equation of evolution, chosen so that a statistical average over initial condition restores the usual predictions of quantum mechanics. There is nevertheless a case where an additional variable emerges almost spontaneously, in an unique way, from the quantum formalism: the spontaneous appearance of relative phase between two highly populated Fock states (Bose-Einstein condensates). The general physical phenomenon was discussed long ago by Anderson¹⁴, with more emphasis on spontaneous symmetry breaking in phase transitions than additional variables in quantum mechanics. Later several authors used various formalisms, often borrowed from quantum optics, to give more detailed calculations^{15,20}. The approach used in Ref. 21 is slightly different since it shows how a simple conservation rule, the conservation of particle number, can naturally be expressed through an integral over the “conjugate” variable, the relative phase Φ of the two states. The probability of any sequence of results then appears as a sum over this new variable, exactly as in theories with additional variables. Moreover, each time a measurement is performed, the state vector projection postulate provides a new initial state, which changes the Φ distribution; it turns out that the change of this probability distribution can be obtained very easily for any sequence of measurements. In other words, one has access to the evolution of the distribution function of the additional variable under the effect of one or more successive quantum measurements. This is what we study in the present article; for the sake of simplicity, we limit ourselves to the limit of large occupation numbers, a case in which the Bell theorem does not predict any incompatibility between quantum mechanics and local realism, so that locality will not be an issue here.

Additional variables in quantum mechanics are often called “hidden variables” for historical reasons. Nevertheless, J. Bell pointed out how inappropriate this name is (“Absurdly, these theories are known as hidden variable theories....”)²², pointing out that the name

would be more appropriate for the standard wave function of quantum mechanics. Indeed, in an interference experiment, for instance, these additional variables are not hidden but actually directly observed in the result of the individual experiments. On the other hand, the wave function or state vector can be reconstructed only indirectly by statistical analysis after many measurements. This is why we will tend to avoid the words “hidden variables” and rather speak of “additional variables” here.

II. PHASE IN SPIN STATES

Suppose we have particles with two internal states, either real spin 1/2 or pseudo-spins as in the case of two hyperfine states. If we have two stationary clouds of Bose particles with N_+ spin-up, and N_- spin-down, particles along a z -axis, the initial state is

$$|\Psi\rangle = |N_+, N_-\rangle, \quad (1)$$

a Fock state in spin space. We want to measure the occurrences of a sequence of spin measurements in the transverse xy -plane, at a series of azimuthal angles, $\phi_1, \phi_2, \dots, \phi_m$, resulting in the sequence of results $\{\eta_i\}$, either up (+) or down (−) along the angles:

$$\eta_1 = \pm 1; \eta_2 = \pm 1; \dots \eta_m = \pm 1. \quad (2)$$

Here we present a simplified calculation of the probabilities, which completely ignores orbital variables; a more precise calculation is given in Appendix A and Ref. 21. We have a set of angular momentum variables given in terms of the destruction operators a for particles up, and b for down, along a z -axis. The number operator is then

$$n = a^\dagger a + b^\dagger b, \quad (3)$$

with the angular momentum variables

$$\begin{aligned} \sigma_z &= a^\dagger a - b^\dagger b, \\ \sigma_x &= a^\dagger b + b^\dagger a, \\ \sigma_y &= i(b^\dagger a - a^\dagger b). \end{aligned} \quad (4)$$

The expectation value of the operator

$$\begin{aligned} p_\eta(\phi_i) &= \frac{1}{2N} [n + \eta (\cos \phi_i \sigma_x + \sin \phi_i \sigma_y)] \\ &= \frac{1}{2N} [n + \eta (e^{i\phi} b^\dagger a + e^{-i\phi} a^\dagger b)] \end{aligned} \quad (5)$$

gives the probability of finding a spin with component η along the angle ϕ_i in the transverse plane. (To see the connection between this operator and the probability, see Appendix A or Ref. 21.) Suppose one measures a single spin along a transverse axis at angle ϕ_1 starting in the state $|\Psi\rangle$ quoted above. The probability of finding spin with result η_1 is easily seen to be

$$P_1(\phi_1) = \langle N_+, N_- | \frac{1}{2N} [n + \eta_1 (e^{i\phi_1} b^\dagger a + e^{-i\phi_1} a^\dagger b)] | N_+, N_- \rangle = \frac{1}{2} \quad (6)$$

as expected. However, if immediately after, one measures a second particle along a different transverse axis ϕ_2 then a straightforward calculation gives the probability of the sequence $\{\eta_1, \eta_2\}$ to be

$$\begin{aligned} P_2(\phi_1, \phi_2) &= \langle N_+, N_- | p_{\eta_2}(\phi_2) p_{\eta_1}(\phi_1) | N_+, N_- \rangle \\ &= \frac{1}{4} \left[1 + \eta_1 \eta_2 \frac{x^2}{2} \cos(\phi_1 - \phi_2) \right], \end{aligned} \quad (7)$$

where $x = 2\sqrt{N_+ N_-}/N$ and $N = N_+ + N_-$. Having found the first particle up or down along ϕ_1 affects the result of the second measurement along ϕ_2 . The two measurements are correlated by boson statistics. It is possible to write this last result in an instructive way as

$$P_2(\phi_1, \phi_2) = \frac{1}{4} \int_0^{2\pi} \frac{d\Phi}{2\pi} (1 + x\eta_1 \cos(\phi_1 - \Phi)) (1 + x\eta_2 \cos(\phi_2 - \Phi)), \quad (8)$$

as one can verify by doing the integration. It is remarkable that this form of the probability for a sequence of m such measurements along transverse axes $\phi_1, \phi_2, \dots, \phi_m$ persists²¹:

$$P_m \sim \int_0^{2\pi} \frac{d\Phi}{2\pi} \prod_{i=1}^m [1 + x\eta_i \cos(\phi_i - \Phi)]. \quad (9)$$

This result just quoted assumes all measurements are done in the transverse plane. However, measurements could also be done of spin up and down along an arbitrary axis at angles (θ_i, ϕ_i) . The generalization of Ref. 21 to this case is described in Appendix A. The derivation there, when specified to all $\theta_i = \pi/2$ and uniform orbital variables, reduces to Eq. (9) as expected.

The form of Eq. (9) is quite interesting. Suppose we had started out with a system polarized partially (at a fraction x) along the transverse direction Φ ; then the resulting probability for finding a set of spins up or down along the set of angles $\{\phi_i\}$ would be Eq. (9) but *without* the integration over Φ . Since we started out knowing the numbers of particles in longitudinal states, all transverse phases must be present equally in the initial state as represented by the integral over the transverse phase in Eq. (9).

We can look at the expression of Eq. (9) in a somewhat different way: The probability that the η in the m th spin measurement is ± 1 , after a sequence of results $\{\eta_i\}$, is

$$P_m(\pm) \sim \int_0^{2\pi} d\Phi g_m(\Phi) (1 \pm x \cos(\phi_m - \Phi)) \quad (10)$$

where the m th measurement is made only in the transverse plane at the angle ϕ_m . In this we have

$$g_m(\Phi) = \prod_{i=1}^{m-1} (1 + x\eta_i \cos(\phi_i - \Phi)). \quad (11)$$

The function $g_m(\Phi)$, as we will see by explicit simulation, peaks up, after a sufficiently large number $m - 1$ of measurements, at some value of phase, call it Φ_0 . Thus subsequent measurements will appear as if the the system of particles had, after just $m - 1$ measurements (with $m \ll N$), been prepared with a set polarization phase angle. (Of course, if we repeated the experiment, starting again from the same initial state, a different phase would emerge and indeed it is random in a series of such experiments.) Because particle number and phase are conjugate variables, the original state of known particle number has, after m measurements, morphed into a state of relatively well-known phase, but with the number of particles up or down along z much less certain (although the total number of particles remains known).

We start with $|\Psi\rangle = |N_+, N_-\rangle$. Our first measurement along some azimuthal angle ϕ produces the new state

$$|\Psi_1\rangle = \frac{1}{2}(n + \eta(e^{i\phi}b^\dagger a + e^{-i\phi}a^\dagger b)) |N_+, N_-\rangle. \quad (12)$$

It is clear that this process produces a mixture of states $|N_+, N_-\rangle$, $|N_+ + 1, N_- - 1\rangle$, and $|N_+ - 1, N_- + 1\rangle$. Each subsequent measurement produces a further mixing of number states so that number becomes less certain. Its conjugate, phase, becomes less uncertain.

As an alternative view one might think of the phase as having been there all along, but temporarily hidden from view, with experiments continually clarifying its value. In such a view one integrates probabilities over all possible values of an additional variable introduced to “complete” quantum mechanics, as we find in Eqs. (9) or (10). The additional quantum variable is this “emerging” phase angle.

In the rest of this section we confine our discussions to the simplified case of $N_+ = N_- = N/2$, or $x = 1$. Let us now Fourier transform $g_m(\Phi)$ to write

$$g_m(\Phi) = a_0^m + \sum_{q=1}^{\infty} [a_q^m \cos(q\Phi) + b_q^m \sin(q\Phi)]. \quad (13)$$

In Eq. (10), only the $q = 1$ term contributes, so that

$$P_m(\pm) = \frac{1}{2} \left[1 \pm \left(\frac{a_1^m}{2a_0^m} \cos \phi_m + \frac{b_1^m}{2a_0^m} \sin \phi_m \right) \right]. \quad (14)$$

With this result we can define two parameters that characterize the the results of the m th measurement. These parameters are Φ_m and α_m (or A_m) given by

$$\cos \Phi_m = \frac{a_1^m}{\sqrt{(a_1^m)^2 + (b_1^m)^2}}; \quad \sin \Phi_m = \frac{b_1^m}{\sqrt{(a_1^m)^2 + (b_1^m)^2}}; \quad \sin \alpha_m = A_m = \frac{\sqrt{(a_1^m)^2 + (b_1^m)^2}}{2a_0^m}. \quad (15)$$

(Because P_m is a probability, $A_m \leq 1$ and we can write A_m as a sine.) We obtain

$$P_m(\pm) = \frac{1}{2} [1 \pm \sin \alpha_m (\cos \phi_m \cos \Phi_m + \sin \phi_m \sin \Phi_m)]. \quad (16)$$

Consider a single spin polarized as some space angle (β, γ) and assume that a measurement is performed along a transverse direction ϕ_m . The probability of finding a $+$ result is given by the well-known expression

$$|\pm \langle \phi_m | \beta, \gamma \rangle|^2 = \frac{1}{2} [1 \pm \sin \beta (\cos \phi_m \cos \gamma + \sin \phi_m \sin \gamma)], \quad (17)$$

which has exactly the same form as Eq. (16) if $\beta = \alpha_m$, $\gamma = \Phi_m$. Actually the two expressions are equal whenever the “spin” lies on a cone of directions around the measurement direction ϕ_m containing this particular direction. We show this “cone of equal probability” (CEP) in Fig. 1 with a spin at arbitrary β, γ on the cone.

What this calculation shows is that two different points of view are possible. At each measurement step, all the effects of the previous measurements are contained in the distribution function $g_m(\Phi)$; in this first point of view, the system is described by a statistical mixtures of spins polarized in transverse directions. But one obtains the same probabilities for the next measurement by replacing this statistical mixture by a single pure spin state, fully polarized along directions $\beta = \alpha_m$, $\gamma = \Phi_m$ (or any direction making the same angle with the direction of measurement). A second point of view is therefore possible, where the spin is fully polarized, but in a direction that is, in general, no longer in the transverse plane. For instance, if the distribution $g_m(\Phi)$ has no Φ dependence, the Φ_m dependence of the probabilities disappears, and this spin is polarized in a direction that is perpendicular to the direction of measurement ($\alpha_m = 0$). On the other hand, the Φ_m dependence is maximum when $\alpha_m = \pi/2$ so that the pure spin state lies in the transverse plane.

III. THE AMHERST EXPERIMENT

Ref. 4 reports an experiment that is well-described by our analysis. In Ref. 4 the experiment is treated in terms of a two-component spinor, with each component representing one of the two condensates in a hyperfine state with a well-defined phase. Here we consider the experiment in terms of a Fock state having an up-spin-down-spin ratio the same as the experiment. The Amherst experiment combines two condensates each originating from a different point and claims that the result shows a “spontaneous transverse polarization.” However, what they are able to detect by laser absorption is the existence of each of the longitudinal components. So after mixing the two components they perform a $\pi/2$ tip in order to measure the size of the polarization and its phase. What they see then is an anticorrelated interference pattern in the two components.

We assume a Fock state for the initial mixed-condensate function: $|\Psi\rangle = |N_+, N_-\rangle$, with an arbitrary pre-established x, y, z coordinate system. We introduce a set of transverse coordinates \hat{u}, \hat{w} offset by an angle ϕ relative to the original xy axes:

$$\hat{u} = \cos \phi \hat{x} + \sin \phi \hat{y} \quad (18)$$

$$\hat{w} = -\sin \phi \hat{x} + \cos \phi \hat{y} \quad (19)$$

We want to measure the \hat{u} -component of the spin in multiple simultaneous measurements made along the longitudinal (z) direction. To enable this we do a spin tip of $\pi/2$ around the \hat{w} axis. Then one measures spins along \hat{z} . So the wave function analyzed is

$$|\Psi'\rangle = U |\Psi\rangle = U |N_+, N_-\rangle \quad (20)$$

where

$$U = e^{i\pi\sigma_w/4} \quad (21)$$

and

$$\sigma_w = -\sin \phi \sigma_x + \cos \phi \sigma_y \quad (22)$$

After applying U we make measurements along \hat{z} , that is, we look for the probability given by

$$P_m = \langle \Psi | U^\dagger \prod_{i=1}^m \frac{1}{2N} (n + \eta_i \sigma_z) U | \Psi \rangle \quad (23)$$

But this is precisely equivalent to the relation

$$P_m = \langle \Psi | \prod_{i=1}^m \frac{1}{2N} (n + \eta_i U^\dagger \sigma_z U) | \Psi \rangle \quad (24)$$

But we have

$$U^\dagger \sigma_z U = \sin \phi \sigma_y + \cos \phi \sigma_x \quad (25)$$

so that

$$P_m = \langle N_+, N_- | \prod_{i=1}^m \frac{1}{2N} (n + \eta_i (\sin \phi \sigma_y + \cos \phi \sigma_x)) | N_+, N_- \rangle \quad (26)$$

$$= \frac{1}{2^m} \int_0^{2\pi} d\Phi g_m(\Phi) (1 + \eta_m x \cos(\phi - \Phi)) \quad (27)$$

where the last line follows from the discussion of the previous section. We have seen that if we make simultaneous measurements over the whole cloud of particles g_m ultimately peaks sharply at a particular phase Φ_0 , so that

$$P_m(\eta_m) \approx \frac{1}{2} (1 + \eta_m x \cos(\phi - \Phi_0)) \quad (28)$$

which is just the result given in Eq. (6) of Ref. 4. What this shows is that the up and down measurements will be anticorrelated in phase. Ref. 4 uses this anticorrelation in phase in the *spatial* interference patterns of the two detected clouds. That reference assumed two point sources of the two bosonic clouds released from traps. The discussion of Appendix A does indeed include a spatial phase; if we use $\theta_i = \pi/2$ there, we find we find that a spatial phase $\xi(r)$ should be added to the argument of the cosine in Eq. (28), where $\xi(r) = \arg[u_a(\mathbf{r})/u_b(\mathbf{r})]$ and $u_a(\mathbf{r})$ and $u_b(\mathbf{r})$ are the single particle wave functions describing the two condensates. An order of magnitude of the behavior of the interference fringes can be derived by assuming we are allowed to substitute simple one-dimensional spreading Gaussian wave packets for $u_a(\mathbf{r})$ and $u_b(\mathbf{r})$. (Appendix A does not explicitly mention time dependence in the wave functions but that inclusion is straightforward.) When we do this we find that the time-dependent phase is of order $\xi(r, t) = md^2/\hbar t$, where d is the separation of the centers of the two wave packets, m the particle mass, and t is the time after the initially narrow packets have been spreading. This feature of time-dependent fringes is assumed in the Amherst experiment as it was in Ref. 23. A complete derivation of this fringe result is given by Wallis et al.²⁴

Our interpretation of the Amherst experiment shows the ambiguity of interpretation that can arise in such an experiment. The interpretation given by Ref. 4 is that the spontaneous

polarization existed in the transverse plane before the ninety degree tip took place. But did it? Before the longitudinal measurements, did Φ_0 exist? One might consider it an additional variable that was already there, but needed to be brought out by experiment. Or one can say it did not exist; the wave function was a linear combination of all such phases and was collapsed by longitudinal measurement to the final value Φ_0 found in the end. Either interpretation works.

IV. NUMERICAL SIMULATION

The physics becomes clearer if we do a numerical simulation of the measurements. The first spin result is chosen randomly up or down along ϕ_1 . To choose from the probability P_m at each subsequent stage ($m = 2, 3, \dots$) we simply pick a random number p from 0 to 1. If $p < P_m(+)$, then $\eta_m = +1$; if $p > P_m(+)$, then $\eta_m = -1$.

The first set of experiments is performed with all measurements done at the same angle $\phi_i = 0$. However, we find that to gain any more information about the emerging phase angle we must switch measurement angles.

A. Experiment with constant direction of measurement.

Our results are shown in the first figures for a run of 300 trials with all $\phi_i \equiv \phi_1 = 0$. There is no plot of the azimuthal angle Φ_m because generally in the case of a constant measurement angle, Φ_m will be equal to ϕ_1 or $\phi_1 + \pi$ for *every* iteration. This is easy to understand physically by a symmetry argument: with a constant direction of measurement, there is no way to distinguish between spins polarized in two directions that are symmetrical with respect to the direction of measurement in the transverse plane. With $\phi_1 = 0$, (or consider the symmetry in terms of $\Phi' = \Phi - \phi_1$), $g_m(\Phi)$ must be a symmetric function around $\Phi = 0$; by Eqs. (13) and (15) we see $b_1^m = 0$, $\sin \Phi_m = 0$, and so $\Phi_m = 0$ or π . For an alternative view of the same result, look at Eq. (16) in the case of all ϕ_m identically equal to ϕ_1 . This equation is of the form

$$P_m(\pm) = \frac{1}{2} [1 \pm \sin \alpha_m \cos(\phi_1 - \Phi_m)] \quad (29)$$

But every cosine in Eq. (10) is a function of $\Phi - \phi_1$, and so the integral is independent of ϕ_1 , as one finds by changing integration variable to $\Phi - \phi_1$. From Eq. (29) this implies that

$\Phi_m - \phi_1 = \text{constant}$, which we show in Appendix B must be 0 or π .

Let m_{\pm} be the number of spins found with $\eta = \pm 1$ along ϕ_1 . We must always have just $P_m(+)=\frac{1}{2}(1\pm\sin\alpha_m)$. Since we anticipate physically that $P_m(+)\cong m_+/(m_++m_-)$ for large m , the plus sign occurs when $m_+>m_-$ and the minus sign in the opposite case. In this constant ϕ_1 case, the variable $A_m=\sin\alpha_m$ goes to some unpredictable random positive value as seen in Fig. 2. (As it does so, it has slightly curved trajectories followed by small jumps: the trajectories occur during a series of identical η values; a jump happens when the opposite η eventually occurs. We explain this peculiar behavior in Appendix C.) Fig. 3 shows $g_{300}(\Phi)$ versus Φ (as well as the earlier and wider g_{10} and g_{150}). It peaks up sharply at *two* locations, near $\pm\Phi_0$ with $\Phi_0=0.73$, symmetrically situated around azimuthal measurement angle $\phi_1=0$; this is exactly what we should expect, as mentioned above, since, in keeping the same measurement angle, the probability is identical for spins symmetrically located to the sides of measurement angle.

There is another piece of data from the run, the number of η 's of each sign. We find that there were $m_+=262$ up spins and $m_-=38$ down spins in the experiment. When $m_+>m_-$ as we have here, we have approximately

$$\frac{1}{2}(1+\sin\alpha_m)\cong\frac{m_+}{m} \quad (30)$$

with $m=m_++m_-$. Solving we get $\sin\alpha=0.75$, which is very close to what we get from the limiting value in Fig. 2. In Appendix C we show that one can do the g integral analytically for constant measurement angle, and the actual results for $\sin\alpha$ is remarkably simple, namely

$$\sin\alpha_m=\frac{|m_+-m_-|}{m+1} \text{ (exact result for constant } \phi_m\text{).} \quad (31)$$

Numerically this is 0.74. For large m the values of Eqs. (30) and (31) are identical since the 1 in Eq. (31) is then negligible.

The above results of $\alpha_m\rightarrow\text{constant}$, and $\Phi_m=0$, seem to imply that the ‘‘hidden polarization direction,’’ whose orientation we are trying to determine, is at zero azimuthal angle and either above or below the transverse plane at *polar* angle α_m . This angle in turn is related to the angles $\pm\Phi_0$ of the peaks of $g_m(\Phi)$ through the cone of equal probability (CEP) of Fig. 1 The cone opening angle is Φ_0 and the polar angle of the cone is the complement $\alpha=\pi/2-\Phi_0$. A general position on the CEP around the measurement angle $\phi_1=0$ obeys

$$P(\pm)=|\pm\langle 0|\beta,\gamma\rangle|^2=\frac{1}{2}[1\pm\sin\beta\cos\gamma]=\frac{1}{2}[1\pm\sin\alpha]$$

$$= \frac{1}{2} \left[1 \pm \sin \left(\frac{\pi}{2} - \Phi_0 \right) \right] = \frac{1}{2} [1 \pm \cos \Phi_0] \quad (32)$$

Thus all we can say about the hidden-spin angle so far is that $\sin \beta \cos \gamma = \sin \alpha = \cos \Phi_0$. We could have $(\beta, \gamma) = (\alpha, 0)$, or $(\beta, \gamma) = (\pi/2, \Phi_0)$ or somewhere else on the cone, but we cannot tell yet which it is. The distribution $g(\Phi)$ peaks at the two places where the CEP crosses the transverse plane.

We can analytically show the double peaking property of $g(\Phi)$ in the case where all measurement angles ϕ_i are equal, say, to zero. Ref. 18 shows how this function has two equal sharp maxima in the range we consider. For completeness we repeat this analysis in Appendix D, getting a Gaussian approximation about each maximum. For large numbers of measurements these Gaussians act as delta-functions at the two angles $\pm \Phi_0$ centered on $\phi = 0$, as we have found in the experiment. Since there are two delta-functions then we find from Eq. (10) that

$$P_m(+) = \frac{1}{2} [(1 + \cos(+\Phi_0)) + (1 + \cos(-\Phi_0))] = \frac{1}{2} (1 + \cos(\Phi_0)). \quad (33)$$

From Eq. (72) in Appendix D, this is

$$P_m(+) = \cos^2(\Phi_0/2) = \frac{m_+}{m}. \quad (34)$$

Of course, this is the same final value we got for $P_m(+)$ above in Eq. (30). We also confirm the relation between α and Φ_0 :

$$\begin{aligned} \cos \Phi_0 &= \sin \alpha \\ \Phi_0 &= \pi/2 - \alpha \end{aligned} \quad (35)$$

as we found above by considering the CEP. As far as the general hidden direction (β, γ) is concerned, all we can say is $\sin \beta \cos \gamma = \cos \Phi_0$ with some ambiguity as to signs or $\pi/2$'s in the angles.

Let us see how this all works out in our experiment. In our first experiment we have $\cos^2(\Phi_0/2) = 262/300 = 0.873$ so that $\Phi_0 = 0.73$. Thus the peaks of g will be at ± 0.73 rad as we have found experimentally and is shown in Fig. 3.

Can we determine *both* the unknowns β and γ from measurements and so remove the ambiguity between the two sides $\pm \Phi_0$ of the cone? The only possible way to do this is to use other measurement angles. If we continue to measure only in the transverse plane,

however, it seems likely we will determine only a combination of β and γ and not both; we would need to go out of the transverse plane to get both. We now consider changes in measurement angle ϕ_1 .

B. Changing the measurement angle:

Suppose we now pick a $\phi_{m+1} \cong +\Phi_0$, (we continue to take the original constant ϕ_1 to be zero), that is, we measure as close to the angle of one of the peaks as we can in the next measurement. We might miss it by δ . What this does is to eliminate completely (or almost) one of the peaks. We show this in Fig. 4. When working at a single angle we did not know on which side of the measurement direction the emerging polarization was. By moving in that direction (or away from it), we do determine the side. We can see this analytically by using the Gaussian approximation developed in Appendix D for the first m iterations. If we move to $+\Phi_0$ then the value of $g_{m+1}(\Phi)$ is

$$\begin{aligned} g_{m+1}(\Phi) &\sim \left[e^{-\frac{1}{2}m(\Phi-\Phi_0)^2} + e^{-\frac{1}{2}m(\Phi+\Phi_0)^2} \right] (1 + \eta_{m+1} \cos(\Phi - \Phi_0 + \delta)) \\ &\approx (1 + \eta_{m+1} \cos \delta) e^{-\frac{1}{2}m(\Phi-\Phi_0)^2} + (1 + \eta_{m+1} \cos(2\Phi_0 - \delta)) e^{-\frac{1}{2}m(\Phi+\Phi_0)^2} \end{aligned} \quad (36)$$

where δ is our measurement inaccuracy. Now if it turned out that $\eta_{m+1} = -1$ we will have most likely made the wrong choice (because if we are close to the correct angle, it is most likely that we will get an $+1$ result) and the wrong peak will be almost completely *eliminated*. If $\eta_{m+1} = +1$, then the correct peak will be emphasized by 2 and the wrong peak given a smaller coefficient. As Fig. 4 shows, it works with just a few measurements (15 in this case) at the new angle -0.73 . We now know on which side of 0 the azimuthal angle lies.

C. Iterations and Convergence:

Next consider what continuing to measure m' more times at this new angle produces. If we have done a good guess at what the polarization angle is then we will get mostly up spin results and as factor containing two peaks from these last m' measurements (with very small separation 2δ) near Φ_0 . Then we will have

$$g_{m+m'}(\Phi) \sim \left[e^{-\frac{1}{2}m(\Phi-\Phi_0)^2} + e^{-\frac{1}{2}m(\Phi+\Phi_0)^2} \right] \left[e^{-\frac{1}{2}m'(\Phi-\Phi_0+\delta)^2} + e^{-\frac{1}{2}m'(\Phi-\Phi_0-\delta)^2} \right]$$

$$\sim 2e^{-\frac{1}{2}(m+m')(\Phi-\Phi_0)^2}. \quad (37)$$

We get a sharpening of the peak. (If δ is too large we might still have two very closely-spaced peaks near Φ_0 .)

Suppose we now have only the one peak after m iterations and it is near $\Phi = +\Phi_0$. That is,

$$g_m(\Phi) \sim e^{-\frac{1}{2}m(\Phi-\Phi_0)^2} \quad (38)$$

This result implies that the mean deviation in the measurements should go as $\sqrt{1/m}$. We Fourier transform this Gaussian to find

$$a_1^m = 2a_0^m e^{-\frac{1}{2m}} \cos \Phi_0; \quad b_1^m = 2a_0^m e^{-\frac{1}{2m}} \sin \Phi_0 \quad (39)$$

so that

$$\tan \Phi_m = \tan \Phi_0; \quad A_m = e^{-\frac{1}{2m}}. \quad (40)$$

and if we continue to make other measurements near this same angle $\Phi = \Phi_0 + \delta_m$, where δ_m is the error in our m th guess about the exact position of Φ_0 , then

$$\begin{aligned} P(+) &= \frac{1}{2} \left[1 + e^{-\frac{1}{2m}} (\cos(\Phi_0 + \delta_m) \cos \Phi_0 + \sin(\Phi_0 + \delta_m) \sin \Phi_0) \right] \\ &\approx \frac{1}{2} \left[1 + e^{-\frac{1}{2m}} (1 + \delta_m \sin \Phi_0 \cos \Phi_0) \right] \approx \frac{1}{2} \left[1 + e^{-\frac{1}{2m}} \right] \rightarrow 1. \end{aligned} \quad (41)$$

The equivalent *simpleminded* point of view is that the spin that was originally at polar angle $\alpha = \Phi_0$ and zero azimuthal angle is *now* is at polar angle $\alpha \approx \pi/2$ and azimuthal angle $+\Phi_0$. But this is still the equivalent for purposes of measurement to a (half) cone of possible “real” 3D positions.

Eqs. (38) and (40) make explicit predictions of how the width of the peak and the amplitude will proceed with measurement number. In order to test those approximate forms let us set up the double peak in 10 measurements, produce a single peak by measuring near one peak angle for just 20 steps and then go back to the original measurement direction $\phi_m = 0$ for a few hundred measurements. In starting anew we develop a different random phase, of course. The results are given in Figs. 5-7. The approximate equations work very well.

For these last measurements, the Fourier transform of Eq. (39) is valid and using it in Eq. (14) with $\phi_m = 0$ we find

$$P_m(+) = \frac{1}{2} \left[1 + \frac{a_1^m}{2a_0^m} \right] = \frac{1}{2} \left[1 + e^{-\frac{1}{2m}} (\cos \Phi_0) \right]. \quad (42)$$

Comparing with the more general point of view at unknown 3D emerging phase angle (β, γ) , given by Eq. (17) we get

$$\sin \beta \cos \gamma = e^{-\frac{1}{2m}} \cos \Phi_0 \quad (43)$$

We might have $\beta = \Phi_0$ and $\gamma = 0$ or $\beta = \pi/2$ and $\gamma = \Phi_0$ but we can never “know” absolutely. (*Indeed in conventional quantum mechanics the wave function is a mixture of all possible phase angles that give the same probability $P(+)$.*) Staying in the transverse plane never yields both the space angles, just this combination. We have now found the maximal information on the emerging phase angle that the present set of measurements can offer. Appendix A discusses how to extend the analysis to angles out of the transverse plane. However, we do not extend the simulation to that case here.

V. CONCLUSIONS

We have presented a simulated experiment where two Bose condensates, one with spin up and the other with spin down, have been allowed to interfere. The standard quantum mechanical view is that a Fock state $|N_+, N_- \rangle$ is a linear combination of phase states. As we make a series of measurements of spin orientation we develop a state that is a mixture of such Fock states having varying numbers of up and down spins, but with constant total number of spins. As we proceed the state becomes a narrower mixture of phase states and the experiment gradually changes the state into nearly just one particular phase state. In conventional quantum mechanics, the measurement process is considered to have created the final phase value by continual wave function collapse. However, as one does the experiment, one may have an equally appealing additional-variable view that the phase emerging was built-in all along and the experiment simply revealed what it was. For the experimentalist, one view works just as well as the other. The formalism developed in Ref. 21 and generalized in Appendix A is particularly appropriate for showing this equivalence since it expresses the results of measurements on a Fock up-down state through an integral over the “conjugate” variable, the relative phase Φ of the two states. The probability of any sequence of results then appears as a sum over the phase, exactly as in theories with additional variables. Each measurement produces a new initial state, with a new Φ distribution; so that the change of this probability distribution can be obtained very easily for any sequence of measurements as we have done in our simulation. Thus we have been able to observe the emergence of

the additional variable under the effect of successive quantum measurements. The Amherst experiment is found to be an ideal example of an actual experiment along these lines.

LKB is UMR 8552 de l'ENS, du CNRS and de l'Universit Pierre et Marie Curie.

VI. APPENDICES

A. Extension to spin measurement at arbitrary directions

In this section we generalize the calculations of Sec. II and Ref. 21, where the directions of spin measurements were assumed to be in the transverse plane; we now assume that the directions are arbitrary. Instead of a single angle ϕ_i to characterize each measurement, we then need two angles θ_i and ϕ_i . (It is more convenient to come back to the standard notation and keep θ_i for the polar angle; ϕ_i therefore now replaces the notation θ_i of Ref. 21.) We also re-introduce orbital variables, which were ignored in Sec. II. We call $|\alpha\rangle$ and $|\beta\rangle$ the two spins states (up and down) and $\Psi_{\alpha,\beta}(\mathbf{r})$ the corresponding field operators. The spin component along the direction of measurement is:

$$\sigma_{\theta,\phi}(\mathbf{r}) = \cos \theta \left[\Psi_{\alpha}^{\dagger}(\mathbf{r})\Psi_{\alpha}(\mathbf{r}) - \Psi_{\beta}^{\dagger}(\mathbf{r})\Psi_{\beta}(\mathbf{r}) \right] + \sin \theta \left[e^{-i\phi} \Psi_{\alpha}^{\dagger}(\mathbf{r})\Psi_{\beta}(\mathbf{r}) + e^{i\phi} \Psi_{\beta}^{\dagger}(\mathbf{r})\Psi_{\alpha}(\mathbf{r}) \right] \quad (44)$$

and the projector²⁶ over the spin eigenstates:

$$P_{\eta} = \frac{1}{2} [n(\mathbf{r}) + \eta \sigma_{\theta,\phi}(\mathbf{r})], \quad (45)$$

with $\eta = \pm 1$ and the local density is defined by:

$$n(\mathbf{r}) = \Psi_{\alpha}^{\dagger}(\mathbf{r})\Psi_{\alpha}(\mathbf{r}) + \Psi_{\beta}^{\dagger}(\mathbf{r})\Psi_{\beta}(\mathbf{r}). \quad (46)$$

The projector is then proportional to:

$$\begin{aligned} P_{\eta}(\mathbf{r};\theta,\phi) &\sim [1 + \eta \cos \theta] \Psi_{\alpha}^{\dagger}(\mathbf{r})\Psi_{\alpha}(\mathbf{r}) + [1 - \eta \cos \theta] \Psi_{\beta}^{\dagger}(\mathbf{r})\Psi_{\beta}(\mathbf{r}) \\ &+ \eta \sin \theta \left[e^{-i\phi} \Psi_{\alpha}^{\dagger}(\mathbf{r})\Psi_{\beta}(\mathbf{r}) + e^{i\phi} \Psi_{\beta}^{\dagger}(\mathbf{r})\Psi_{\alpha}(\mathbf{r}) \right]. \end{aligned} \quad (47)$$

As in §3.1 of Ref. 21, we assume that the system of spin particles is initially in the state:

$$|\Psi_0\rangle = |N_a : u_a, \alpha; N_b : u_b, \beta\rangle \quad (48)$$

where the orbital states correspond to the wave functions (normalized to one):

$$\langle \mathbf{r} | u_{a,b} \rangle = u_{a,b}(\mathbf{r}). \quad (49)$$

The initial system is therefore simply the juxtaposition of a large number N_a of particles condensed into the wave function $u_a(\mathbf{r})$ with a large number N_b of particles condensed into the wave function $u_b(\mathbf{r})$. We now assume that M spin measurements are performed at points $\mathbf{r}_1, \mathbf{r}_2, \dots, \mathbf{r}_m$ in spin direction defined by angles $(\theta_1, \phi_1), (\theta_2, \phi_2), \dots, (\theta_m, \phi_m)$ and calculate the probability for obtaining a series of results $\eta_1, \eta_2, \dots, \eta_m$ (all η 's are equal to ± 1). The corresponding probability is the average value in state $|\Psi_0\rangle$ of a product of P projectors $P_{\eta_i}(\theta_i, \phi_i)$.

The rest of the calculation is very similar to that Ref. 21; the only difference being the presence of the terms in $\eta \cos \theta$ in Eq. (47) and the $\sin \theta$ factor, which do not change much the calculation. The same considerations apply on the conservation of the number of particles in each state and, in the limit where $m \ll N_a, N_b$, we can express this conservation through an integral over a phase Φ . The probability then becomes proportional to the expression:

$$\begin{aligned} & \int_0^{2\pi} \frac{d\Phi}{2\pi} \prod_{i=1}^m \left\{ [1 + \eta_i \cos \theta_i] N_a |u_a(\mathbf{r}_i)|^2 + [1 - \eta_i \cos \theta_i] N_b |u_b(\mathbf{r}_i)|^2 \right. \\ & \left. + \eta_i \sin \theta_i \sqrt{N_a N_b} [u_a(\mathbf{r}_i) u_b^*(\mathbf{r}_i) e^{i(\phi_i - \Phi)} + \text{c.c.}] \right\}, \end{aligned} \quad (50)$$

where c.c. stands for “complex conjugate.” The second line of this result can also be written as

$$+ 2\eta_i \sin \theta_i \sqrt{N_a N_b} |u_a(\mathbf{r}_i)| |u_b(\mathbf{r}_i)| \cos [\xi(\mathbf{r}_i) - \phi_i - \Phi] \quad (51)$$

where $\xi(\mathbf{r})$ is the relative phase of the two wave functions of the condensates:

$$\xi(r) = \arg [u_a(\mathbf{r})/u_b(\mathbf{r})]. \quad (52)$$

This second line contains all the Φ dependence of the probabilities; in other words it is the only origin of correlations between different measurements. It also contains the \mathbf{r} dependence of the probability, which produces the fringes in space.

The discussion of §§ 1.1 and 3.1 of Ref. 21 shows that effect of the i -th measurement on the Φ distribution is merely to multiply this distribution by a function $D_i(\Phi)$ that is nothing but the content of the i -th curly bracket in Eq. (50) (with a normalization constant that is unimportant for our discussion here). This multiplication provides the evolution of

the information on the relative phase Φ that is obtained by this measurement. Whatever measurement parameters $\mathbf{r}_i, (\theta_i, \phi_i)$ are arbitrarily chosen, the multiplying function $D_i(\Phi)$ is always the sum of a constant (first line of (50)) plus a sinusoidal variation given by (51). The former depends on \mathbf{r}_i and θ_i only, with the \mathbf{r}_i dependence involving only the densities of probabilities associated with the condensed states; the latter depends also on ϕ_i as well as the relative phase of the two states. Both depend in general on the result of the measurement η_i , as opposed to the situation for measurement in transverse directions only ($\theta_i = \pi/2$).

If, for instance, we assume that $\eta_i = +1$, the maximum and the minimum of the contribution to the probability of the i -th measurement can be written as

$$\left\{ \sqrt{N_a} |u_a(\mathbf{r}_i)| \cos \frac{\theta_i}{2} \pm \sqrt{N_b} |u_b(\mathbf{r}_i)| \sin \frac{\theta_i}{2} \right\}^2. \quad (53)$$

The best contrast will therefore be obtained if the minimum vanishes, that is if:

$$\tan \frac{\theta_i}{2} = \sqrt{\frac{N_a}{N_b}} \left| \frac{u_a(\mathbf{r}_i)}{u_b(\mathbf{r}_i)} \right|. \quad (54)$$

This provides the optimum value of θ_i for each measurement position \mathbf{r} if $\eta_i = +1$. But, if $\eta_i = -1$, it is easy to see that $\cos \theta_i/2$ and $\sin \theta_i/2$ are interchanged in (53), so that the the right hand side of (54) now provides the inverse of $\tan \theta_i/2$; the optimum value of θ_i corresponding to the two possible results are therefore symmetrical with respect to the horizontal plane.

As a consequence, the choice of the optimum value of θ_i is not easy in general, since it depends on the random result of an experiment that is not yet known when the apparatus is adjusted. If, nevertheless, one can locate the position \mathbf{r}_i of the measurement at a point where the two bosonic fields have the same intensity:

$$N_a |u_a(\mathbf{r}_i)|^2 = N_b |u_b(\mathbf{r}_i)|^2 \quad (55)$$

the dilemma disappears: the optimum value of θ_i is $\pi/2$, corresponding to a measurement performed in a direction of the transverse plane. In this case, the flexibility introduced by the new parameter θ_i is useless. Nevertheless, condition Eq. (55) is not necessarily easy to meet, and may even be impossible for some configurations. Then, the optimization of the polar direction of measurement becomes relevant, but only if one already has a good idea in advance of what the most likely value of Φ is, so that with an appropriate choice of φ_i it is possible to infer what the result η_i of the next measurement will be with a good probability.

The conclusion is then that the flexibility introduced by θ_i may be useful, but only after a series of measurements has already been performed, so that Φ is already reasonably well known.

B. Proof that $\Phi_m = \phi \pmod{\pi}$ for measurement along a single direction

Consider the situation in which the measurement angle ϕ remains the same in every measurement. Then we can Fourier transform

$$g_m(\Phi) = \prod_{i=1}^{m-1} (1 + \eta_i \cos(\Phi - \phi)). \quad (56)$$

in a series in $\cos(\phi - \Phi)$ rather than in $\cos \Phi$ and $\sin \Phi$. That is

$$g_m(\Phi) = a_0^m + \sum_q c_q^m \cos(q(\Phi - \phi)) = a_0^m + \sum_q \left(c_q^m \cos \Phi \cos \phi + c_q^m \sin \Phi \sin \phi \right). \quad (57)$$

from which we find

$$P_n(+) \sim 1 + \frac{c_1^m}{2a_0^m}. \quad (58)$$

By comparison with Eq. (13) we see that

$$a_1^m = c_1^m \cos \phi; \quad b_1^m = c_1^m \sin \phi, \quad (59)$$

which, by Eq. (15), shows that $\tan \Phi_m = \tan \phi$ or

$$\Phi_m = \phi \text{ or } \phi + \pi, \quad (60)$$

and that $c_1^m/2a_0^m = \sin \alpha_m \cos(\Phi_m - \phi) = \pm \sin \alpha_m$. This also gives

$$P_m(+) = \frac{m_+}{m} = \frac{1}{2}(1 \pm \sin \alpha_m). \quad (61)$$

where the $+$ sign occurs with $m_+ > m_-$ and the $-$ sign in the opposite case so that $\sin \alpha_m$ is positive.

C. Analytic results for constant measurement angle

When all measurement angles are the same value we can with full generality take that angle equal to zero and write

$$\begin{aligned} g_m(\Phi) &= \prod_{i=1}^{m-1} (1 + \eta_i \cos(\Phi)) = (1 + \cos(\Phi))^{m_+} (1 - \cos(\Phi))^{m_-} \\ &= 2^m \left(\cos \frac{\Phi}{2} \right)^{m_+} \left(\sin \frac{\Phi}{2} \right)^{m_-} \end{aligned} \quad (62)$$

Then the Fourier transforms are found from integral tables²⁵ to be

$$\begin{aligned} a_0^m &= \frac{2^m}{2\pi} \int_0^{2\pi} d\Phi \left(\cos \frac{\Phi}{2} \right)^{m_+} \left(\sin \frac{\Phi}{2} \right)^{m_-} \\ &= \frac{2^m}{\pi} \frac{\Gamma(m_+ + \frac{1}{2}) \Gamma(m_- + \frac{1}{2})}{\Gamma(m+1)} \end{aligned} \quad (63)$$

$$\begin{aligned} a_1^m &= \frac{2^m}{\pi} \int_0^{2\pi} d\Phi \left(\cos \frac{\Phi}{2} \right)^{m_+} \left(\sin \frac{\Phi}{2} \right)^{m_-} \cos \Phi \\ &= \frac{2^{m+1}}{\pi} \frac{\Gamma(m_+ + \frac{3}{2}) \Gamma(m_- + \frac{1}{2}) - \Gamma(m_+ + \frac{1}{2}) \Gamma(m_- + \frac{3}{2})}{\Gamma(m+2)} \end{aligned} \quad (64)$$

with $b_1^m = 0$ by symmetry. Taking the ration of these and using the definition of $\sin \alpha_m$ gives

$$\sin \alpha_m = \frac{|a_1^m|}{2a_0^m} = \frac{|m_+ - m_-|}{m+1}. \quad (65)$$

This result allows us to understand the behavior of A_m as seen in Fig. 1. We notice that the plot has small upward curves followed by abrupt downward jumps. We find that the upward sweep is a sequence of all $\eta = 1$ results while a downward jump is a single $\eta = -1$. Suppose, as occurs in the figure that m_+ is considerably larger than m_- . Then when a new up spin result occurs the change in A_m is given by

$$\Delta_+ = \frac{m_+ + 1 - m_-}{m+2} - \frac{m_+ - m_-}{m+1} = \frac{2m_- + 1}{(m+2)(m+1)} \quad (66)$$

while, if a down spin occurs in the measurement, the change in this quantity is

$$\Delta_- = \frac{m_+ - m_- - 1}{m+2} - \frac{m_+ - m_-}{m+1} = -\frac{2m_+ + 1}{(m+2)(m+1)} \quad (67)$$

The second quantity, the jump down, is much greater in magnitude than the previous upward move, giving the peculiar shape of the curve.

D. The peaks in $g(\Phi)$ for the spin phase

Here we analyze $g(\Phi)$ in the case of all equal measurement axes $\phi_i = \phi$ to show it has two sharp peaks. We can take the single measurement angle to be zero with generality (or work with $\Phi' = \Phi - \phi$). The location of these peaks corresponds to what we have found numerically. Write $g(\Phi)$ in the half-angle form

$$g(\Phi) = \left(\cos^2 [(\Phi)/2] \right)^{m_+} \left(\sin^2 [(\Phi)/2] \right)^{m_-}. \quad (68)$$

Set the derivative of the logarithm of this to zero to determine the position of the maxima.

$$\frac{d \ln g(\Phi)}{d\Phi} = -m_+ \frac{\sin [(\Phi)/2]}{\cos [(\Phi)/2]} + m_- \frac{\cos [(\Phi)/2]}{\sin [(\Phi)/2]} = 0, \quad (69)$$

which is equivalent to

$$\cos^2 [(\Phi)/2] = \frac{m_+}{m}. \quad (70)$$

This equation has two solutions in the range $0 \leq \Phi < 2\pi$. These are at

$$\Phi = \pm\Phi_0 \quad (71)$$

where Φ_0 is in the range $[0, \pi]$ or

$$\cos^2 [\Phi_0/2] = \frac{m_+}{m}. \quad (72)$$

Thus the two peaks occur symmetrically about the value of $\Phi = 0$ just as we have found “experimentally.” Correspondingly we have

$$\sin^2 [\Phi_0/2] = \frac{m_-}{m}. \quad (73)$$

We get a Gaussian approximation to g by Taylor expanding $\ln g$ about $\pm\Phi_0$. We use

$$\left. \frac{d^2 \ln g(\Phi)}{d\Phi^2} \right|_{\Phi_0} = -m, \quad (74)$$

so that¹⁸

$$g(\Phi) = \left(\frac{m_+}{m}\right)^{m_+} \left(\frac{m_-}{m}\right)^{m_-} \left[e^{-\frac{1}{2}m(\Phi-\Phi_0)^2} + e^{-\frac{1}{2}m(\Phi+\Phi_0)^2} \right]. \quad (75)$$

For large m these act like delta-functions.

¹ H. J. Lewandowski, D. M. Harber, D. L. Whitaker, and E. A. Cornell, Phys. Rev. Lett. **88**, 070403 (2002).

² J. M. McGuirk, H. L. Lewandowski, D. M. Harper, T. Nikuni, J. E. Williams, and E. A. Cornell, Phys. Rev. Lett. **89**, 090402 (2002).

³ M. Jammer, “The conceptual development of quantum mechanics”, McGraw Hill, 2nd ed. (1989).

⁴ Mark H. Wheeler, Kevin M. Mertes, Jessie D. Erwin, and David S. Hall, Phys. Rev. Lett. **93**, 170402-1 (2004).

- ⁵ L. de Broglie, in “Rapport au Vème congrès de physique Solvay”, Gauthier Villars, Paris (1930).
- ⁶ D. Bohm, Phys. Rev. **85**, 166 and 180 (1952).
- ⁷ A. Einstein, N. Rosen and B. Podolsky, Phys. Rev. **47**, 777 (1935); or in “Quantum theory of measurement”, J.A. Wheeler and W.H. Zurek eds, Princeton University Press (1983), 138.
- ⁸ J. S. Bell, “On the Einstein-Podolsky-Rosen paradox”, Physics **1**, 195 (1964); reprinted in “Quantum theory of measurement”, J.A. Wheeler and W.H. Zurek eds, Princeton Univ. Press (1983), 396.
- ⁹ J. S. Bell, “Speakable and unspeakable in quantum mechanics”, Cambridge University Press (1987).
- ¹⁰ The so called “efficiency loophole” has not yet been closed, but very few physicists now think that quantum mechanics will fail in an experiment that is free of this loophole.
- ¹¹ N. D. Mermin, Rev. Mod. Phys. **65**, 803 (1993).
- ¹² F. Laloë, Am. J. Phys. **69**, 655 (2001).
- ¹³ S. Goldstein, “Quantum Theory without observers”, Physics Today **51**, 42 (March 1998) and 38 (April 1998).
- ¹⁴ P. W. Anderson, Rev. Mod. Phys. **38**, 298 (1966); P.W. Anderson, “Basic notions in condensed matter physics”, Benjamin-Cummins (1984).
- ¹⁵ J. Javanainen and Sun Mi Yoo, Phys. Rev. Lett. **76**, 161 (1996).
- ¹⁶ T. Wong, M.J. Collett and D. F. Walls, Phys. Rev. **A 54**, R3718 (1996).
- ¹⁷ J. I. Cirac, C. W. Gardiner, M. Naraschewski and P. Zoller, Phys. Rev. **A 54**, R3714 (1996).
- ¹⁸ Y. Castin and J. Dalibard, Phys. Rev. **A 55**, 4330 (1997).
- ¹⁹ K. M. Imer, Phys. Rev. **A 55**, 3195 (1997).
- ²⁰ K. M. Imer, J. Mod. Opt. **44**, 1937 (1997).
- ²¹ F. Laloë, Eur. Phys. J. **33**, 87 (2005).
- ²² J. S. Bell, “Are there quantum jumps?” in Ref. 9.
- ²³ M. R. Andrews, C. G. Townsend, H.-J. Miesner, D. S. Durfee, D. M. Kurn, and W. Ketterle, Science **275**, 637 (1997).
- ²⁴ H. Wallis, A. Röhrl, M. Naraschewski, and A. Schenzle, Phys. Rev. **A 53**, 2109 (1997).
- ²⁵ M. Abramowitz and I. A. Stegun, *Handbook of Mathematical Functions*, Dover Publications (1972), Sec. 6.2.
- ²⁶ Strictly speaking, the projectors contain an integral over a small domain $\Delta_{\mathbf{r}}$, which we do not

write explicitly here for the sake of simplicity It is assumed that the domains are sufficiently small to make the average number of particles in them much less than 1. See the discussion in § 1.1 of Ref. 21, after equation (5).

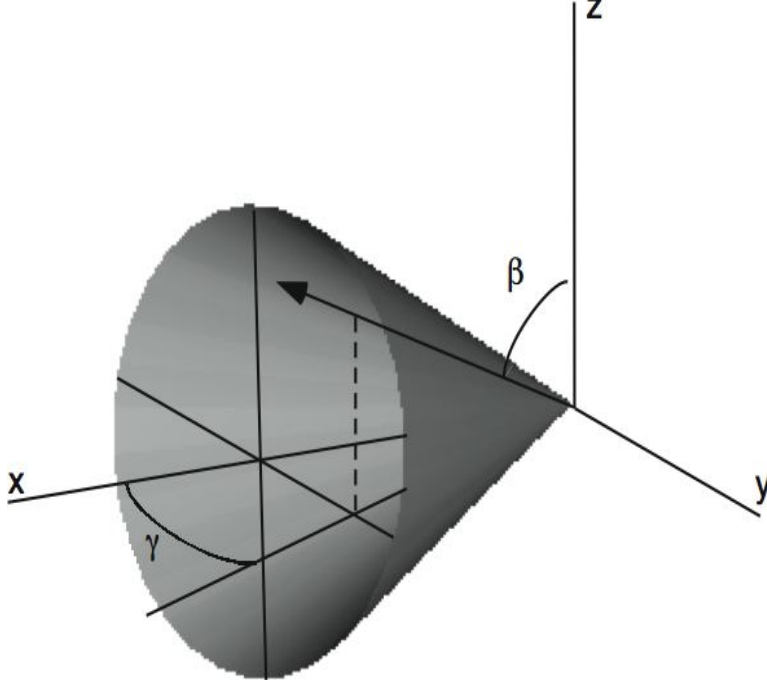


FIG. 1: The cone of equal probability. Any spin at angles β, γ on this cone will give the same probability of being up along the measurement axis, taken as x in this figure.

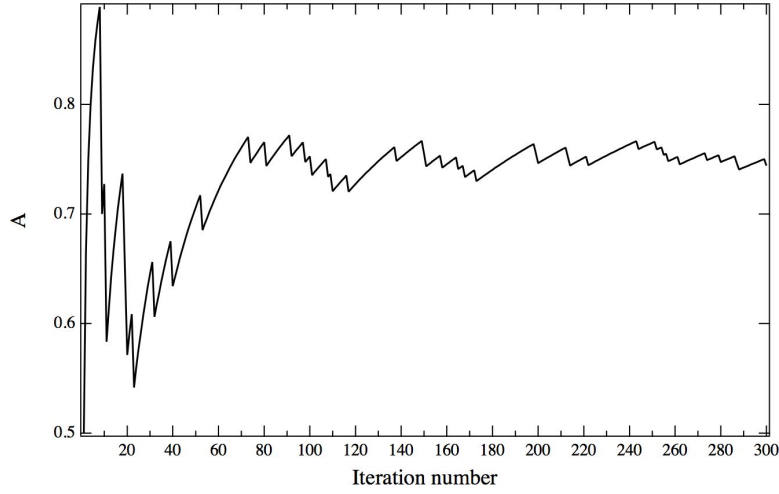


FIG. 2: The amplitude $A = \sin \alpha$ as a function of iteration step when all measurements have been made at a single angle. The final asymptotic value is random.

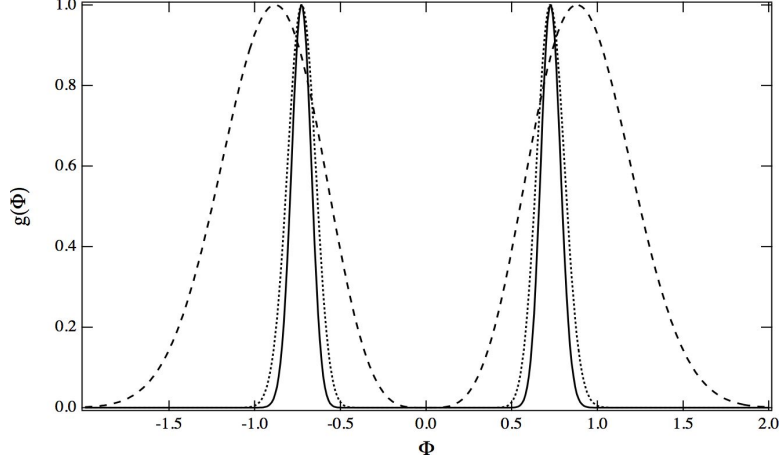


FIG. 3: The angular distribution $g(\Phi)$ as a function of angle for three iteration step lengths, 10 steps (dashed line), 150 steps (dotted line), and 300 steps (solid line). For a single measuring angle this always has two equal peaks corresponding to the intersection of the spin cone with the transverse plane. The peaks narrow with step length.

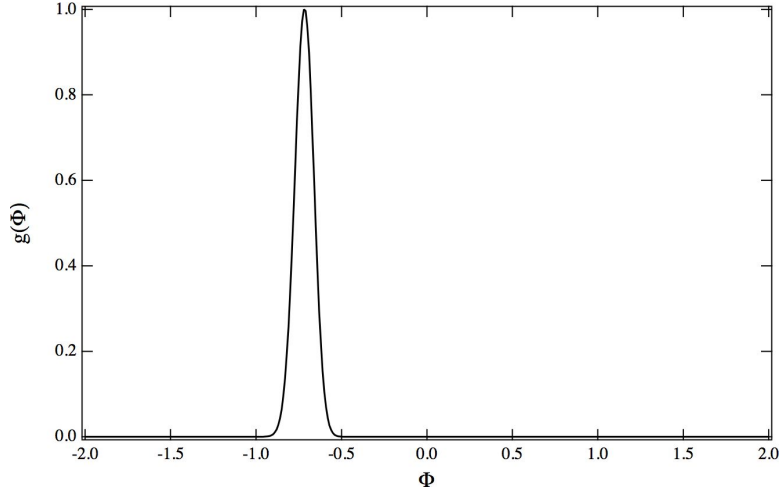


FIG. 4: Typical $g(\Phi)$ after the second peak has been eliminated by a few measurements at the positive peak.

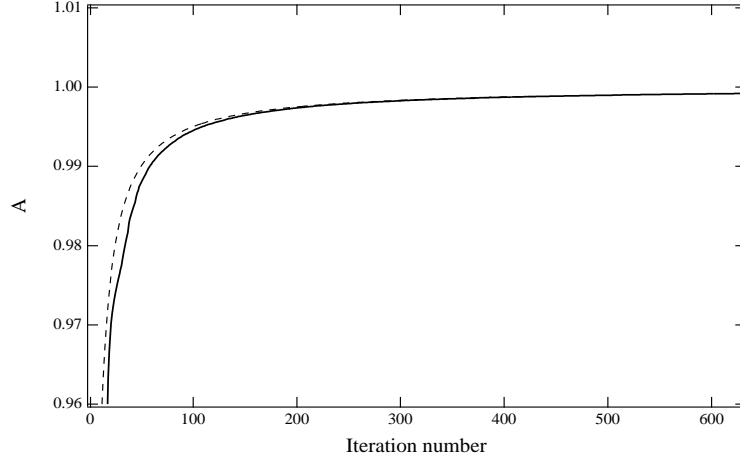


FIG. 5: The amplitude A_m as a function of iteration step when all measurements, after eliminating the second peak of $g(\Phi)$ early on, are back at the original measurement angle $\phi_1 = 0$. The dotted line is the approximation $e^{-1/2m}$.

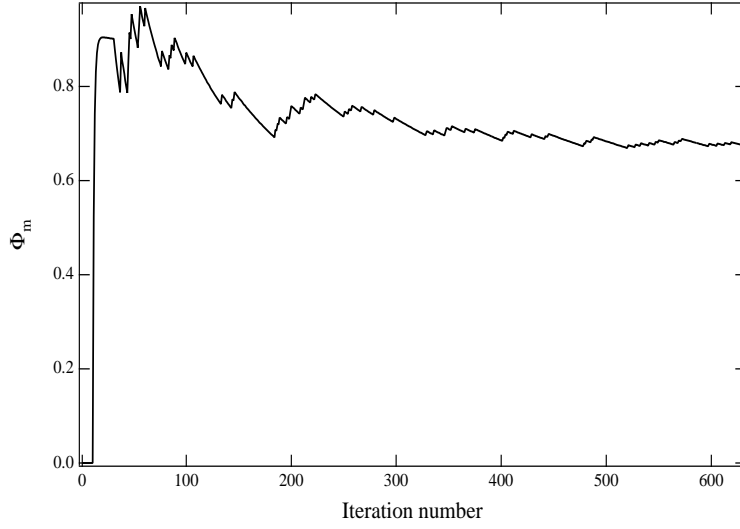


FIG. 6: The azimuthal angle $\Phi_m \approx \Phi_0$ as a function of iteration step when all measurements, after eliminating the second peak of $g(\Phi)$ early on, are back at the original measurement angle $\phi_1 = 0$.

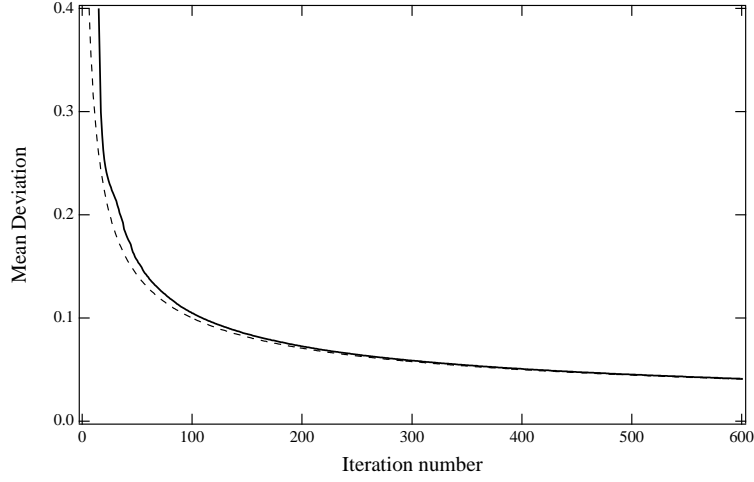


FIG. 7: The mean deviation (width of $g(\Phi)$) as a function of iteration step when all measurements, after eliminating the second peak of $g(\Phi)$ early on, are back at the original measurement angle $\phi_1 = 0$. The dotted line is the approximate form $1/\sqrt{m}$